740 Ma vase-shaped microfossils from Yukon, Canada: Implications for Neoproterozoic chronology and biostratigraphy

Justin V. Strauss[1], Alan D. Rooney[1], Francis A. Macdonald[1], Alan D. Brandon[2], and Andrew H. Knoll[1]
[1]Department of Earth and Planetary Sciences, Harvard University, Cambridge, Massachusetts 02138, USA
[2]Department of Earth and Atmospheric Sciences, University of Houston, Houston, Texas, 77204, USA

ABSTRACT

Biostratigraphy underpins the Phanerozoic time scale, but its application to pre-Ediacaran strata has remained limited because Proterozoic taxa commonly have long or unknown stratigraphic ranges, poorly understood taphonomic constraints, and/or inadequate geochronological context. Here we report the discovery of abundant vase-shaped microfossils from the Callison Lake dolostone of the Coal Creek inlier (Yukon, Canada) that highlight the potential for biostratigraphic correlation of Neoproterozoic successions using species-level assemblage zones of limited duration. The fossiliferous horizon, dated here by Re-Os geochronology at 739.9 ± 6.1 Ma, shares multiple species-level taxa with a well-characterized assemblage from the Chuar Group of the Grand Canyon (Arizona, USA), dated by U-Pb on zircon from an interbedded tuff at 742 ± 6 Ma. The overlapping age and species assemblages from these two deposits suggest biostratigraphic utility, at least within Neoproterozoic basins of Laurentia, and perhaps globally. The new Re-Os age also confirms the timing of the Islay $\delta^{13}C_{carbonate}$ anomaly in northwestern Canada, which predates the onset of the Sturtian glaciation by >15 m.y. Together these data provide global calibration of sedimentary, paleontological, and geochemical records on the eve of profound environmental and evolutionary change.

INTRODUCTION

Neoproterozoic sedimentary deposits of western North America record large fluctuations in global biogeochemical cycles (e.g., Narbonne et al., 1994; Karlstrom et al., 2000; Halverson et al., 2005), the diversification of multiple eukaryotic clades (e.g., Porter and Knoll, 2000; Samuelsson and Butterfield, 2001; Cohen and Knoll, 2012), the fragmentation of Rodinia accompanied by localized mafic volcanism (e.g., Jefferson and Parrish, 1989; Prave, 1999; Macdonald et al., 2010), and multiple global glaciations (e.g., Aitken, 1991; Hoffman et al., 1998). Understanding the causal relationships among these events requires accurate stratigraphic correlation in the context of geochronologically constrained age models. However, the geographically disparate Neoproterozoic sedimentary records along the length of western North America have yet to be clearly linked in time and space due a paucity of radiometric age constraints, non-unique chemostratigraphic ties, abundant synsedimentary tectonism and associated lateral facies change, and a lack of biostratigraphically useful microfossils. Correlations have been proposed for pre-glacial Neoproterozoic strata in the southwestern United States (e.g., Dehler et al., 2001, 2010), but these schemes have not been extended to the rich sedimentary archives of northwest Canada, due primarily to a lack of age control. Here we document new vase-shaped microfossil (VSM) assemblages from Yukon, Canada, that are indistinguishable in taxonomic composition and age from those described from the Chuar Group of the Grand Canyon (Arizona, USA) and successions of similar age worldwide (Porter and Knoll, 2000; Porter et al., 2003). Given their abundance, diversity, preservation, and time-calibrated record, VSMs could represent the first temporally well-resolved biostratigraphic assemblage zone for pre-Ediacaran strata, opening a new window for regional and global stratigraphic correlation that goes beyond previous broad morphoclass-based biostratigraphic comparisons.

STRATIGRAPHY

The Coal Creek inlier in the Ogilvie Mountains (Yukon, Canada) hosts an ~3-km-thick sequence of ca. 780–540 Ma Windermere Supergroup strata (Fig. 1; Mustard and Roots, 1997). The Mount Harper Group consists of three informal units; in stratigraphically ascending order, these are (1) the Callison Lake dolostone, an ~400-m-thick mixed siliciclastic and carbonate deposit; (2) the Mount Harper conglomerate, an ~1100-m-thick rift-related clastic succession; and (3) the Mount Harper volcanics, an ~1200-m-thick intermediate to mafic volcanic complex (Mustard and Roots, 1997; Macdonald et al., 2010). Age constraints on the Mount Harper Group are provided by U-Pb chemical abrasion–thermal ionization mass spectrometry (CA-TIMS) ages on zircon of 811.51 ± 0.25 Ma from a tuff in the underlying Fifteenmile Group,

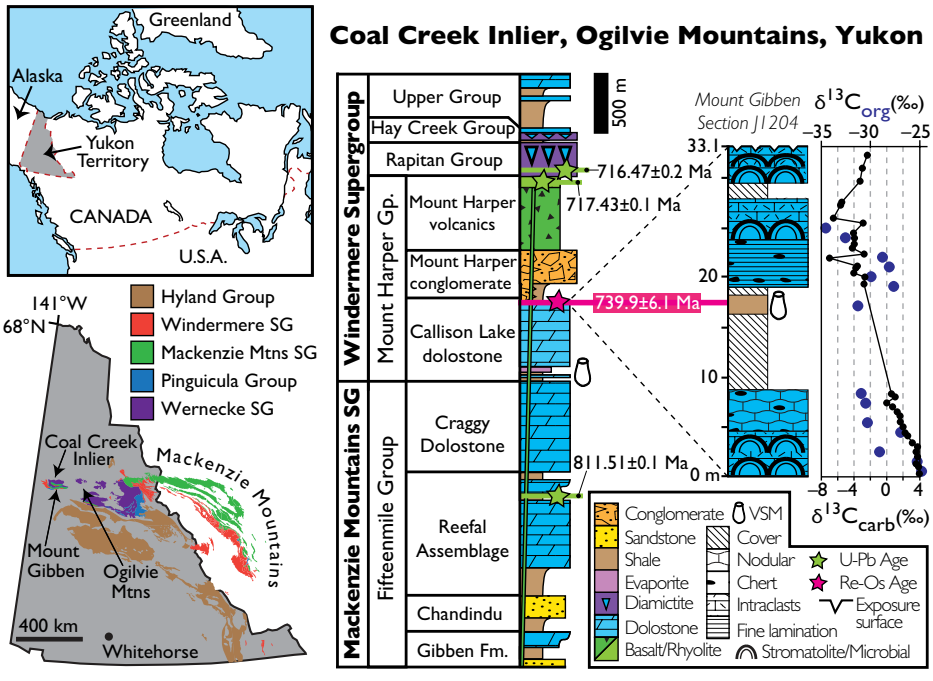

Figure 1. Simplified map locations and schematic lithostratigraphy of the Coal Creek inlier, Yukon, Canada. Vase-shaped microfossils (VSMs) described herein are from Callison Lake dolostone. Measured section J1204 highlights location of fossil and Re-Os age horizon, as well as bounding $\delta^{13}C_{carb}$ and $\delta^{13}C_{org}$ (blue data points) data from the Islay anomaly. Geologic map of Yukon is adapted from Wheeler and McFeely (1991). Abbreviations: SG—Supergroup; Gp.—Group; Fm.—Formation; Mtns—mountains.

GEOLOGY, August 2014; v. 42; no. 8; p. 659–662; Data Repository item 2014244 | doi:10.1130/G35736.1 | Published online 9 June 2014

717.43 ± 0.14 Ma from rhyolite in the upper member of the Mount Harper volcanics, and 716.47 ± 0.24 Ma from a tuff interbedded with diamictite correlated with the glacially influenced Rapitan Group in the Mackenzie Mountains (Fig. 1; Macdonald et al., 2010).

The lower Mount Harper Group records mixed marine and terrestrial deposition intimately associated with an east-west–trending, syndepositional north-side-down fault scarp that outlines the remnants of a Proterozoic half-graben (Mustard and Roots, 1997). Basal deposits of the Callison Lake dolostone unconformably overlie brecciated and silicified strata of the Fifteenmile Group, and consist of an ~4–30-m-thick interval of sandstone, siltstone, and discontinuous beds of quartz and chert pebble conglomerate that transition into ~5–30 m of black to varicolored and mud-cracked shale interbedded with laterally discontinuous stromatolitic bioherms that host poorly preserved VSMs. Basal Callison Lake siliciclastic deposits are sharply overlain by an ~15–100-m-thick medium gray dolostone characterized by pisolitic grainstone, microbial laminae, morphologically diverse stromatolites, evaporite pseudomorphs, intraclast conglomerate, and mechanically bedded dolomicrite and/or dolosiltite, which also contains intercalated black shale composed predominantly of authigenic talc [$Mg_3Si_4O_{10}(OH_2)$] (Tosca et al., 2011). These strata are overlain by 200–300 m of dolostone characterized by abundant microbial lamination, domal stromatolitic bioherms, and cross-bedded oolitic grainstone, with abundant early diagenetic chert. The Callison Lake dolostone culminates with another recessive ~10–40-m-thick unit of fossiliferous black shale, locally silicified and interbedded with stromatolitic and microbial dolostone, that is gradationally to abruptly overlain by sandstone and conglomerate of the Mount Harper conglomerate (Fig. 1). Callison Lake strata record peritidal to shallow subtidal deposition in an episodically restricted marginal marine basin, the subsidence of which was largely driven by regional extension.

PALEONTOLOGY

A diverse VSM assemblage (Fig. 2) occurs in the uppermost organic-rich silicified shale of the Callison Lake dolostone (Fig. 1; section J1204, 16.8–18.2 m). Because of pervasive silicification, the fossils cannot readily be freed from their matrix and so must be evaluated in petrographic thin section. Individual thin sections contain many hundreds of essentially random cross sections through VSMs (Fig. 2A). As in the Chuar Group assemblage (Porter et al., 2003), nearly all preserved fossils are tear-shaped tests characterized by (1) circular outline in transverse section; (2) radially or bilaterally symmetrical form with a rounded aboral pole opposite a tapered oral end with aperture; (3) broad size ranges, from ~20 to 200 µm in length and ~15 to 120 µm in width; (4) morphologically diverse apertures ~10–40 µm wide; and (5) ~1–3-µm-thick test walls. Most sections through Callison Lake specimens do not yield systematically diagnostic characters; however, because the fossils are so abundant, each thin section includes many dozens of individuals that permit species-level comparison to Chuar Group populations (Porter et al., 2003). Thus, we can identify *Melanocyrillium hexodiadema* (Figs. 2A and 2C), *Palaeoarcella athanata* (Fig. 2B), *Bombycion micron* (Fig. 2D), *Bonniea dacruchares* (Fig. 2E), and *Cycliocyrillium torquata* (Fig. 2F), as well as *Bonniea pytinaia*, *C. simplex*, *Hemisphaeriella ornata*, and other long-necked unnamed forms (not illustrated).

All observed VSMs reflect a taphonomic history similar to that of Chuar Group populations; they are siliceous or calcareous internal molds commonly coated with thin layers of pyrite, iron oxide, or organic matter (Fig. 2; Porter and Knoll, 2000). Porter and Knoll (2000) outlined the taphonomic processes that preserved such microfossils and summarized previous interpretations of their biological affinities, making a strong case for viewing Chuar Group VSMs as testate amoebae placed phylogenetically within the Amoebozoa and Rhizaria. As such, these fossils provide our earliest direct evidence of protistan predation, including the evolutionarily important innovation of eukaryvory, the capture and ingestion of other eukaryotic cells (Porter, 2011; Knoll, 2014).

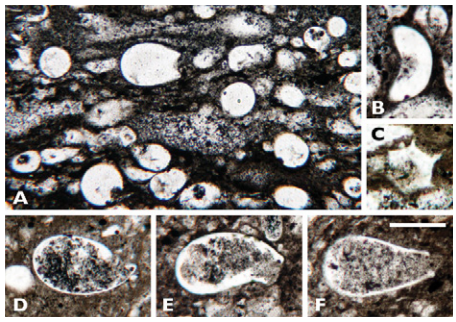

Figure 2. Neoproterozoic vase-shaped microfossils (VSMs) from Callison Lake dolostone, Yukon, Canada. (Slide number and England Finder Coordinates are given for each image.) A: Low-magnification image showing abundance of VSM tests, with centrally located specimen of *Melanocyrillium hexodiadema* (J1204.16.8; K23/0). Scale = 100 µm. B: *Palaeoarcella athanata* (J1204.16.8; H31/1). Scale = 50 µm. C: Cross section of *Melanocyrillium hexodiadema* aperture (F930.15.5; O33/4). Scale = 50 µm. D: *Bombycion micron* (J1204.18.1; H32/2). Scale = 40 µm. E: *Bonniea dacruchares* (J1204.18.1; W31/1). Scale = 50 µm. F: *Cycliocyrillium torquata* (J1204.18.1; L43/1). Scale = 50 µm.

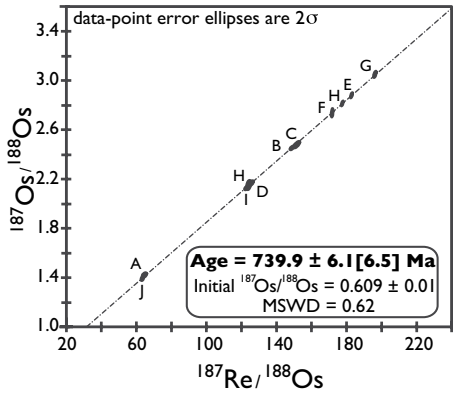

Figure 3. Re-Os isochron for upper Callison Lake dolostone (Yukon, Canada) with an age uncertainty of 6.5 m.y. (in brackets) when uncertainty of ^{187}Re decay constant is included. MSWD—mean square of weighted deviates. Isotope composition and abundance data are presented in the Data Repository (see footnote 1).

GEOCHRONOLOGY

Silicified black shale of the Callison Lake dolostone was collected from a VSM-bearing outcrop near Mount Gibben in the Coal Creek inlier (Fig. 1; section J1204, 16.8–18.2 m). This 2.4-m-thick exposure was sampled at high resolution for Re-Os geochronology, and bounding stromatolitic dolostone was collected at ~1 m resolution for $\delta^{13}C_{carb}$ and $\delta^{13}C_{org}$ chemostratigraphy (Fig. 1; details of the sampling procedure and analytical methods are provided in the GSA Data Repository[1]). A Re-Os age of 739.9 ± 6.1 Ma (±6.5 m.y. if including ^{187}Re decay constant uncertainty; n = 10, mean square of weighted deviates, MSWD = 0.62, 2σ, initial $^{187}Os/^{188}Os$ = 0.609 ± 0.01) was obtained from this horizon (Fig. 3). This Re-Os age is within error of the U-Pb zircon age of 742 ± 6 Ma from a reworked tuff interbedded with VSM-bearing black shale of the upper Chuar Group (Fig. 4), providing a distinct geochronological tie for our paleontological comparisons.

DISCUSSION

Early fragmentation of Rodinia ca. 780–720 Ma generated local tectonism, mafic volcanism, and regional basin subsidence in western North America (e.g., Jefferson and Parrish, 1989; Prave, 1999; Karlstrom et al., 2000). In northwestern Canada, the Mount Harper Group and Coates Lake Group were deposited in a series of narrow, fault-bounded basins between ca.

[1]GSA Data Repository item 2014244, a summary of sampling techniques, detailed analytical methods, data tables containing all isotopic and geochronological data, and a compilation of global vase-shaped microfossil occurrences, is available online at www.geosociety.org/pubs/ft2014.htm, or on request from editing@geosociety.org or Documents Secretary, GSA, P.O. Box 9140, Boulder, CO 80301, USA.

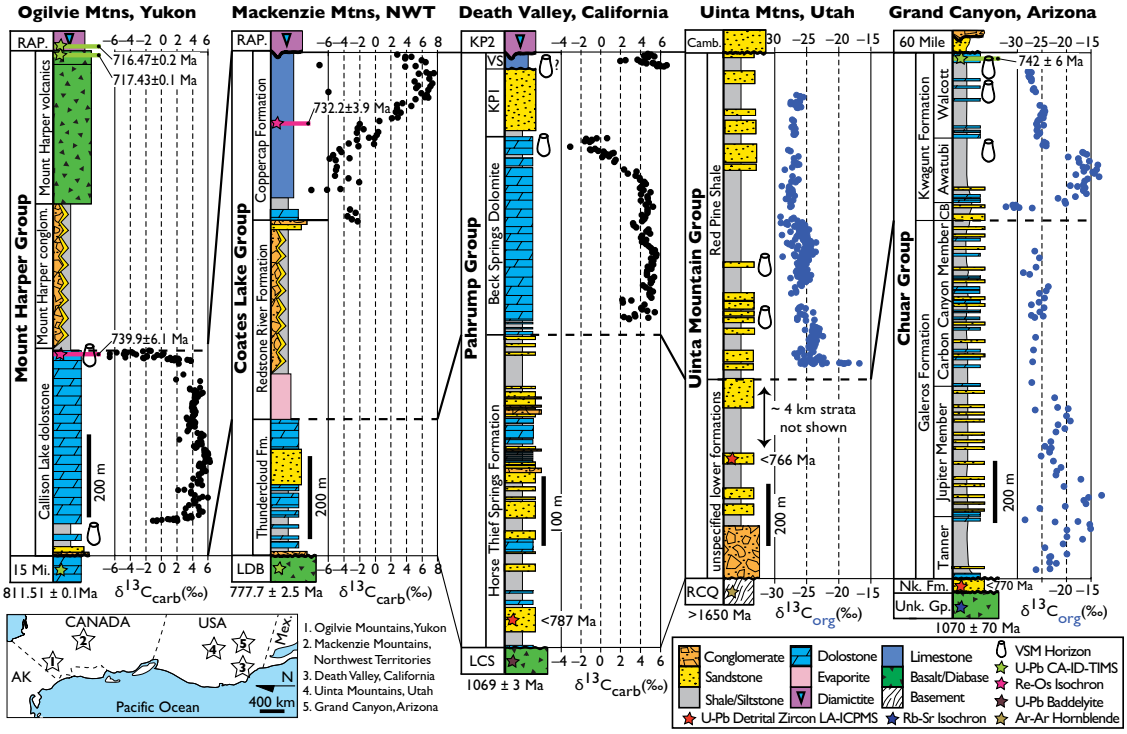

Figure 4. Schematic lithostratigraphy, geochronology, and carbon isotope chemostratigraphy of basal Windermere Supergroup strata from western North America. All $\delta^{13}C_{org}$ data are shown with blue data points. Data are summarized from (1) this paper and Macdonald et al. (2010); (2) Jefferson and Parrish (1989) and Rooney et al. (2014); (3) Macdonald et al. (2013) and Mahon et al. (2014); (4) Dehler et al. (2010) and Nelson et al. (2011); (5) Karlstrom et al. (2000) and Dehler et al. (2010). Numbers correlate to inset map. Abbreviations: AK—Alaska; Mex.—Mexico; carb—carbonate; org—organic; VSM—vase-shaped microfossil; Mtns—Mountains; conglom.—conglomerate; 15 Mi.—Fifteenmile Group; LDB—Little Dal basalt; RAP.—Rapitan Group; KP—Kingston Peak Formation; VS—Virgin Spring limestone; LCS—Lower Crystal Spring Formation; RCQ—Red Creek Quartzite; Camb.—Cambrian; CB—Carbon Butte Member; NK. Fm.—Nankoweap Formation; Unk. Gp.—Unkar Group; LA-ICP-MS—laser ablation–inductively coupled plasma–mass spectrometry; CA-TIMS—chemical abrasion–thermal ionization mass spectrometry.

777 and 720 Ma (Jefferson and Parrish, 1989; Mustard and Roots, 1997). Farther south, the Chuar, Pahrump, and Uinta Mountain groups were also deposited in extensional basins between ca. 780 Ma and 740 Ma (Fig. 4; Timmons et al., 2001; Dehler et al., 2001, 2010). Based on a compilation of previously published carbon isotope chemostratigraphy, the new Re-Os age constraints discussed herein, and the first appearance of VSMs in different basins along the length of the Cordillera, we can begin to correlate these pre-Sturtian basins with confidence throughout western North America (Fig. 4).

Interestingly, all of these ca. 780–720 Ma basins in western North America host VSM assemblages and/or pronounced carbon isotopic fluctuations below Sturtian glacial deposits (Fig. 4), hinting at complex links between tectonics, biogeochemical cycling, and climate (Karlstrom et al., 2000). In conjunction with the U-Pb CA-TIMS zircon ages from the Mount Harper and Rapitan Groups of the Coal Creek inlier and the Re-Os age of 732.2 ± 3.9 Ma within a large negative $\delta^{13}C_{carb}$ anomaly in the Coates Lake Group of the Mackenzie Mountains (Rooney et al., 2014), the Re-Os geochronology and chemostratigraphy presented herein suggest a clear correlation between the Mount Harper Group and Coates Lake Group (Fig. 4). Furthermore, this $\delta^{13}C_{carb}$ isotopic pattern is indistinguishable from that of the Beck Spring Dolomite in Death Valley, which also hosts VSMs in association with a large negative carbon isotope anomaly (Fig. 4; Macdonald et al., 2013). We correlate these $\delta^{13}C_{carb}$ anomalies with the pre-Sturtian Islay anomaly because of their stratigraphic position below glacial deposits and their broad covariance with $\delta^{13}C_{org}$ and lack of covariance with $\delta^{18}O_{carb}$ (Fig. 1; Table DR1 in the Data Repository; Rooney et al. 2014). This $\delta^{13}C_{carb}$ excursion is commonly associated with a distinct recovery to enriched $\delta^{13}C_{carb}$ values prior to the onset of glacial sedimentation (e.g., Prave et al., 2009; Hoffman et al., 2012), clearly seen in the Coates Lake Group but masked by siliciclastic deposits in the Mount Harper Group (Fig. 4). Tziperman et al. (2011) suggested that accelerating eukaryotic diversification led to increased export production, triggering dynamic effects in the carbon cycle due to anaerobic respiration, consumption of CO_2, and the initiation of glaciation. Our data are consistent with this model insofar as it relates the Islay $\delta^{13}C_{carb}$ anomaly to the abundant preservation of diverse VSMs; however, the apparent ~15 m.y. age disparity before the onset of the Sturtian glaciation suggests that any evolutionary influence on the Neoproterozoic Earth system must be interpreted broadly and not specifically in terms of the Islay event. Our new geochronological data sever the proposed link between the Islay anomaly and the onset of global glaciation (Tziperman et al., 2011; Hoffman et al., 2012), unless there are multiple Islay-like $\delta^{13}C_{carb}$ anomalies recorded in ca. 745–716 Ma preglacial strata or an earlier episode of glaciation.

Globally, strata above the Bitter Springs $\delta^{13}C_{carb}$ anomaly (younger than 811 Ma; Macdonald et al., 2010) but below Sturtian glaciogenic rocks are characterized by an increased diversity of eukaryotes that includes morphologically complex acritarchs, diverse VSM populations (see Table DR3 for a summary of global VSM occurrences), complex protistan scales, and a number of simple multicellular and coenocytic taxa (Knoll et al., 2006; Cohen and Knoll, 2012). Of these, VSMs are particularly well suited for biostratigraphic correlation, given their distinctive forms, relative ease of preservation, wide facies distribution, and limited stratigraphic range; they meet the requirements of biostratigraphic index fossils. Previous workers have noted the potential utility of VSMs for Neoproterozoic biostratigraphy (e.g., Knoll and Vidal, 1980; Porter and Knoll, 2000; Dehler et al., 2001); however, these suggestions were based on broad morphoclass comparisons without tight radiometric age constraints. In contrast, we suggest that VSMs in the Callison Lake and Chuar strata constitute a species-level assemblage zone comparable to those used to delimit time in Phanerozoic successions. Traditionally, Proterozoic taxa were held to have long stratigraphic ranges, far different from most Phanerozoic species (Knoll, 1994), but the advent of eukaryote-ingesting predators would be predicted to increase protistan turnover rates, much as carnivory did among Cambrian animals (Knoll, 2014), and this may underpin

the limited stratigraphic longevity inferred for Chuar Group–Callison Lake dolostone VSMs. At most, the Chuar–Callison Lake assemblage zone characterizes an interval comparable in length to a Phanerozoic epoch or period, and our radiometric dates suggest that its duration could have been considerably shorter, more akin to Phanerozoic ages. Lower Callison Lake fossils occur about one-third of the way between the well-characterized upper fossiliferous horizon and a subjacent ca. 811 Ma tuff in the Fifteenmile Group. Consistent with data from other basins (Fig. 4), this suggests that VSMs in general occur through an interval tens of millions of years in duration; but, because of poor preservation, the lower fossils do not provide information on the stratigraphic ranges of individual species. Thus, the new results promise a transition from established Proterozoic biostratigraphic links, where morphoclass correlations are coarse and many of the taxa used to correlate among basins have long ranges, to species-level assemblage zone correlation constrained by radiometric age constraints.

ACKNOWLEDGMENTS

We thank the Yukon Geological Survey, the National Science Foundation (NSF) Graduate Research Fellowship to Strauss; NSF Sedimentary Geology and Paleobiology grant EAR-1148058, and the NASA Astrobiology Institute for financial and logistic support; Fireweed Helicopters for transportation; D. Schrag for the use of the Laboratory for Geochemical Oceanography at Harvard University; C. Roots, G. Halverson, P. Cohen, N. Tosca, E. Sperling, E. Smith, E. Kennedy, and A. Gould for assistance in the field and stimulating discussions; and N. Butterfield, C. Dehler, and an anonymous reviewer for constructive comments.

REFERENCES CITED

Aitken, J.D., 1991, Two Late Proterozoic glaciations, Mackenzie Mountains, northwestern Canada: Geology, v. 19, p. 445–448, doi:10.1130/0091-7613(1991)019<0445:TLPGMM>2.3.CO;2.

Cohen, P.A., and Knoll, A.H., 2012, Scale microfossils from the mid-Neoproterozoic Fifteenmile Group, Yukon Territory: Journal of Paleontology, v. 86, p. 775–800, doi:10.1666/11-138.1.

Dehler, C.M., Elrick, M., Karlstrom, K.E., Smith, G.A., Crossey, L.J., and Timmons, J.M., 2001, Neoproterozoic Chuar Group (~800–742 Ma), Grand Canyon: A record of cyclic marine deposition during global cooling and supercontinent rifting: Sedimentary Geology, v. 141–142, p. 465–499, doi:10.1016/S0037-0738(01)00087-2.

Dehler, C.M., Fanning, C.M., Link, P.K., Kingsbury, E.M., and Rybczynski, D., 2010, Maximum depositional age and provenance of the Uinta Mountain Group and Big Cottonwood Formation, northern Utah: Paleogeography of rifting western Laurentia: Geological Society of America Bulletin, v. 122, p. 1686–1699, doi:10.1130/B30094.1.

Halverson, G.P., Hoffman, P.F., Schrag, D.P., Maloof, A.C., and Rice, A.H.N., 2005, Toward a Neoproterozoic composite carbon isotope record: Geological Society of America Bulletin, v. 117, p. 1181–1207, doi:10.1130/B25630.1.

Hoffman, P.F., Kaufman, A.J., Halverson, G.P., and Schrag, D.P., 1998, A Neoproterozoic Snowball Earth: Science, v. 281, p. 1342–1346, doi:10.1126/science.281.5381.1342.

Hoffman, P.F., Halverson, G.P., Domack, E.W., Maloof, A.C., Swanson-Hysell, N.L., and Cox, G.M., 2012, Cryogenian glaciations on the southern tropical paleomargin of Laurentia (NE Svalbard and East Greenland), and a primary origin for the upper Russøya (Islay) carbon isotope excursion: Precambrian Research, v. 206–207, p. 137–158, doi:10.1016/j.precamres.2012.02.018.

Jefferson, C.W., and Parrish, R., 1989, Late Proterozoic stratigraphy, U-Pb zircon ages, and rift tectonics, Mackenzie Mountains, northwestern Canada: Canadian Journal of Earth Sciences, v. 26, p. 1784–1801, doi:10.1139/e89-151.

Karlstrom, K.E., et al., 2000, Chuar Group of the Grand Canyon: Record of breakup of Rodinia, associated change in the global carbon cycle, and ecosystem expansion by 740 Ma: Geology, v. 28, p. 619–622, doi:10.1130/0091-7613(2000)28<619:CGOTGC>2.0.CO;2.

Knoll, A.H., 1994, Proterozoic and Early Cambrian protists: Evidence for accelerating evolutionary tempo: National Academy of Sciences Proceedings, v. 91, p. 6743–6750, doi:10.1073/pnas.91.15.6743.

Knoll, A.H., 2014, Paleobiological perspectives on early eukaryotic evolution: Cold Spring Harbor Perspectives in Biology, v. 6, 14 p., doi:10.1101/cshperspect.a016121.

Knoll, A.H., and Vidal, G., 1980, Late Proterozoic vase-shaped microfossils from the Visingsö Beds, Sweden: Geologiska Föreningen i Stockholm Förhandlingar, v. 102, p. 207–211, doi:10.1080/11035898009455157.

Knoll, A.H., Javaux, E.J., Hewitt, D., and Cohen, P., 2006, Eukaryotic organisms in Proterozoic oceans: Royal Society of London Philosophical Transactions, ser. B, v. 361, p. 1023–1038, doi:10.1098/rstb.2006.1843.

Macdonald, F.A., Schmitz, M.D., Crowley, J.L., Roots, C.F., Jones, D.S., Maloof, A.C., Strauss, J.V., Cohen, P.A., Johnston, D.T., and Schrag, D.P., 2010, Calibrating the Cryogenian: Science, v. 327, p. 1241–1243, doi:10.1126/science.1183325.

Macdonald, F.A., Prave, A., Petterson, R., Smith, E.F., Pruss, S., Oates, K., Waechter, F., Trotzuk, D., and Fallick, A., 2013, The Laurentian record of Neoproterozoic glaciation, tectonism, and eukaryotic evolution in Death Valley, California: Geological Society of America Bulletin, v. 125, p. 1203–1223, doi:10.1130/B30789.1.

Mahon, R.C., Dehler, C.M., Link, P.K., Karlstrom, K.E., and Gehrels, G.E., 2014, Geochronologic and stratigraphic constraints on the Mesoproterozoic and Neoproterozoic Pahrump Group, Death Valley, California: A record of the assembly, stability, and break of Rodinia: Geological Society of America Bulletin, v. 126, p. 652–664, doi:10.1130/B30956.1.

Mustard, P.S., and Roots, C.F., 1997, Rift-related volcanism, sedimentation, and tectonic setting of the Mount Harper Group, Ogilvie Mountains, Yukon Territory: Geological Survey of Canada Bulletin, v. 492, 92 p., doi:10.4095/208670.

Narbonne, G.M., Kaufman, A.J., and Knoll, A.H., 1994, Integrated chemostratigraphy and biostratigraphy of the Windermere Supergroup, northwestern Canada: Implications for Neoproterozoic correlations and the early evolution of animals: Geological Society of America Bulletin, v. 106, p. 1281–1292, doi:10.1130/0016-7606(1994)106<1281:ICABOT>2.3.CO;2.

Nelson, S.T., Hart, G.L., and Frost, C.D., 2011, A reassessment of Mojavia and a new Cheyenne Belt alignment in the eastern Great Basin: Geosphere, v. 7, p. 513–527, doi:10.1130/GES00595.1.

Porter, S.M., 2011, The rise of predators: Geology, v. 39, p. 607–608, doi:10.1130/focus062011.1.

Porter, S.M., and Knoll, A.H., 2000, Testate amoebae in the Neoproterozoic Era: Evidence from vase-shaped microfossils in the Chuar Group, Grand Canyon: Paleobiology, v. 26, p. 360–385, doi:10.1666/0094-8373(2000)026<0360:TAITNE>2.0.CO;2.

Porter, S.M., Meisterfeld, R., and Knoll, A.H., 2003, Vase-shaped microfossils from the Neoproterozoic Chuar Group, Grand Canyon: A classification guided by modern testate amoebae: Journal of Paleontology, v. 77, p. 409–429, doi:10.1666/0022-3360(2003)077<0409:VMFTNC>2.0.CO;2.

Prave, A.R., 1999, Two diamictites, two cap carbonates, two $\delta^{13}C$ excursions, two rifts: The Neoproterozoic Kingston Peak Formation, Death Valley, California: Geology, v. 27, p. 339–342, doi:10.1130/0091-7613(1999)027<0339:TDTCCT>2.3.CO;2.

Prave, A.R., Fallick, A.E., Thomas, C.W., and Graham, C.M., 2009, A composite C-isotope profile for the Neoproterozoic Dalradian Supergroup of Scotland and Ireland: Geological Society of London Journal, v. 166, p. 129–135, doi:10.1144/0016-76492007-126.

Rooney, A.D., Macdonald, F.A., Strauss, J.V., Dudás, F.O., Hallmann, C., and Selby, D., 2014, Re-Os geochronology and coupled Os-Sr isotope constraints on the Sturtian snowball: National Academy of Sciences Proceedings, v. 111, p. 51–56, doi:10.1073/pnas.1317266110.

Samuelsson, J., and Butterfield, N.J., 2001, Neoproterozoic fossils from the Franklin Mountains, northwestern Canada: Stratigraphic and palaeobiological implications: Precambrian Research, v. 107, p. 235–251, doi:10.1016/S0301-9268(00)00142-X.

Timmons, J.M., Karlstrom, K.E., Dehler, C.M., Geissman, J.W., and Heizler, M.T., 2001, Proterozoic multistage (ca. 1.1. and 0.8 Ga) extension in the Grand Canyon Supergroup and establishment of a northwest- and north-trending tectonic grain in the southwestern United States: Geological Society of America Bulletin, v. 113, p. 163–181, doi:10.1130/0016-7606(2001)113<0163:PMCAGE>2.0.CO;2.

Tosca, N.J., Macdonald, F.A., Strauss, J.V., Johnston, D.T., and Knoll, A.H., 2011, Sedimentary talc in Neoproterozoic carbonate successions: Earth and Planetary Science Letters, v. 306, p. 11–22, doi:10.1016/j.epsl.2011.03.041.

Tziperman, E., Halevy, I., Johnston, D.T., Knoll, A.H., and Schrag, D.P., 2011, Biological induced initiation of Neoproterozoic snowball-Earth events: National Academy of Sciences Proceedings, v. 108, p. 15091–15096, doi:10.1073/pnas.1016361108.

Wheeler, J., and McFeely, P., 1991, Tectonic assemblage map of the Canadian Cordillera and adjacent parts of the United States of America: Geological Survey of Canada A series Map 1712A, scale 1:200,000.

Manuscript received 1 April 2014
Revised manuscript received 13 May 2014
Manuscript accepted 14 May 2014

Printed in USA

DATA REPOSITORY ITEM 2014244

CARBONATE CARBON AND OXYGEN ISOTOPES

We report $\delta^{13}C_{carb}$ and $\delta^{18}O_{carb}$ measurements of 48 samples from sections J1204 and F930 of the Callison Lake Dolostone (Table DR1). These are parallel measured sections (~1-2 m apart) *of the exact same strata* from a small drainage south of Mount Gibben at N64°40'53.6" W139°13'55.6" in the Coal Creek inlier, Yukon Territory, Canada. In Fig. 1 of the manuscript, we present $\delta^{13}C_{carb}$ data solely from J1204 because F930 is a lower resolution repetition of the same section. We use the $\delta^{13}C_{org}$ data from F930 based on very straightforward bed-by-bed correlations combined with matching the same $\delta^{13}C_{carb}$ values (Table DR1).

Carbon ($\delta^{13}C_{carb}$) and oxygen ($\delta^{18}O_{carb}$) isotopic results are reported in per mil notation of $^{13}C/^{12}C$ and $^{18}O/^{16}O$, respectively, relative to the standard VPDB (Value of the Pee-Dee Belemnite). Dolostone samples were cut perpendicular to bedding, polished, and carefully microdilled (~2-10 mg of powder) to avoid secondary veins, cements, and siliciclastic components. Carbonate $\delta^{13}C$ and $\delta^{18}O$ isotopic data were acquired simultaneously on a VG Optima dual inlet isotope ratio mass spectrometer coupled with a VG Isocarb preparation device (Micromass, Milford, MA) in the Laboratory for Geochemical Oceanography at Harvard University. Approximately 1 mg of sample powder was reacted in a common, purified phosphoric acid (H_3PO_4) bath at 90°C. The evolved CO_2 was collected cryogenically and analyzed using an in-house reference gas. Measured data were calibrated to VPDB using the Cararra marble standard. Total analytical errors (1σ) are better than ± 0.1‰ for both $\delta^{13}C$ and $\delta^{18}O$ based on repeat analysis of standards and samples. Increasing the reaction time to eleven minutes for dolomite samples minimized potential "memory effects" resulting from the common acid-bath system, with the total memory effect estimated at <0.1‰ based on reproducibility of standards run directly after samples.

ORGANIC CARBON ISOTOPES

We report $\delta^{13}C_{org}$ measurements from 13 samples of section F930 of the Callison Lake Dolostone (Table DR1). $\delta^{13}C_{org}$ values were obtained from the total organic carbon (TOC) of insoluble residues. Whole rock samples were initially trimmed to remove weathered material and secondary veins and then crushed into a powder in a SPEX 8500 Shatterbox using a hardened steel grinding container and puck. Analyses were performed on large (~10-20g) samples to accommodate low TOC values. Samples were decalcified with concentrated HCl (6N) for 48 hours, buffered back to a neutral pH (>pH5), filtered, and dried. Care was taken to ensure that acid was added and acidification continued until there was absolutely no visible carbonate dissolution so that the analyses would not be affected by contamination from residual inorganic carbon. Homogenized residues were analyzed in the Harvard University Laboratory for Geochemical Oceanography on a Carlo Erba Elemental Analyzer attached to a ThermoFinnigan Delta V configured in continuous flow mode. Samples and standards were bracketed such that our 13 organic carbon analyses (each run in duplicate) were associated with 6 internal standards. These standards, each with known organic carbon contents and isotope values, were used to calibrate TOC contents and isotopic compositions. The mass of insoluble residue was taken as siliciclastic content, and TOC values for the bulk samples were calculated by

combining the carbonate concentration data obtained from the Delta with measurements of the ratio of insoluble residue to original pre-decarbonated powder.

RHENIUM-OSMIUM GEOCHRONOLOGY

Organic-rich (TOC = 1.15–2.5%), vase-shaped microfossil-bearing black shale was sampled from section J1204. Ten samples large enough for Re-Os geochronology (~50-200 g) were collected over an interval of 2.2 m (J1204-16.8–18.2 m) after an ~25 cm deep trench was dug to remove weathered material from the outcrop. Seven of these ten samples (Table DR2: B–H) were collected horizontally from a very thin (<10 cm) vertical interval (17.7 m), as a large horizontal sampling technique is generally used to maximize the spread of $^{187}Re/^{188}Os$ (Kendall et al., 2009). Given the lack of variability from this small horizon, we incorporated three other vertical samples (Table DR2: A, I, and J) to develop our final isochron age (Fig. 3 of manuscript). This 2.2 m interval is sedimentologically identical and the Os*i* values (Table DR2) of every sample is practically indistinguishable from one another.

All of the sample weathered surfaces were removed with a diamond-coated rock saw and samples were then hand-polished using a diamond-plated polishing pad to remove cutting marks and eliminate any potential for contamination from the saw blade. The samples were dried overnight at ~60 °C and then crushed to a fine (~30 μm) powder in a SPEX 8500 Shatterbox using a zirconium grinding container and puck in order to homogenize any Re and Os heterogeneity present in the samples. Re and Os isotopic abundances and compositions were determined at the Department of Earth and Atmospheric Sciences, University of Houston (UH) following methodology developed by van Acken et al. (2012) and Wittig et al. (2013).

0.6 g of sample was digested and equilibrated in 8 ml of $Cr^{VI}O_3$-H_2SO_4 together with a mixed tracer (spike) solution of ^{190}Os and ^{185}Re in carius tubes at 220 °C for 48 hours. Rhenium and osmium was extracted and purified using solvent extraction (NaOH, $(CH_3)_2CO$, and $CHCl_3$,), micro-distillation, anion column chromatography methods, and negative mass spectrometry as outlined by Selby and Creaser (2003) and Cumming et al. (2013). The $Cr^{VI}O_3$-H_2SO_4 digestion method was employed as it has been shown to preferentially liberate hydrogenous Re and Os yielding more accurate and precise age determinations (Selby and Creaser, 2003; Kendall et al., 2004; Rooney et al., 2011). Total procedural blanks during this study were 12.3 ± 0.1 pg and 0.05 ± 0.15 pg for Re and Os respectively, with an average $^{187}Os/^{188}Os$ value of 0.172 ± 0.208 (1σ, n = 3).

Isotopic measurements were performed using the UH ThermoElectron TRITON PLUS mass spectrometer via static Faraday collection for Re and ion-counting using a secondary electron multiplier in peak-hopping mode for Os. In-house Re and Os solutions were continuously analyzed during the course of this study to ensure and monitor long-term mass spectrometer reproducibility. The University of Houston Re standard solution measured on the faraday cups yields an average $^{185}Re/^{187}Re$ value of 0.59827 ± 0.00158 (2σ, n = 10), which is identical to that of (Rooney et al., 2010). The measured difference in $^{185}Re/^{187}Re$ values for the Re solution and the accepted $^{185}Re/^{187}Re$ value (0.5974) (Gramlich et al., 1973) is used to correct the Re sample data. The Os isotope standard solution used at UH is the in-house standard from the University of Maryland. Over the past two years on this Triton, the runs yield a $^{187}Os/^{188}Os$ ratio of

0.11388 ± 0.00116 (2σ, *n* = 41) that is identical, within uncertainty, to the accepted value reported in Brandon et al., (1999).

Uncertainties for $^{187}Re/^{188}Os$ and $^{187}Os/^{188}Os$ are determined by error propagation of uncertainties in Re and Os mass spectrometry measurements, blank abundances and isotopic compositions, spike calibrations, and reproducibility of standard Re and Os isotopic values. The Re-Os isotopic data, 2σ calculated uncertainties for $^{187}Re/^{188}Os$ and $^{187}Os/^{188}Os$, and the associated error correlation function (rho) are regressed to yield a Re-Os date using *Isoplot V. 4.15* with the $\lambda\ ^{187}Re$ constant of $1.666 \times 10^{-11}\ a^{-1}$ (Ludwig, 1980; Smoliar et al., 1996; Ludwig, 2011). Elemental Re and Os abundances for the J1204 samples range from 0.7 to 9.5 ppb, and 61.8 to 357.6 ppt, respectively, with $^{187}Re/^{188}Os$ and $^{187}Os/^{188}Os$ ratios between 63 and 196, and 1.421 and 3.050 respectively (Table DR2). Regression of the isotopic composition data for these samples yields a Model 1 age of 739.9 ± 6.1 Ma (6.5 if the ^{187}Re decay constant uncertainty is included, *n* = 10, Mean Square of Weighted Deviates [MSWD] = 0.62, initial $^{187}Os/^{188}Os = 0.609 \pm 0.01$; Fig. 3).

REFERENCES CITED

Brandon, A.D., Norman, M.D., Walker, R.J., Morgan, J.W., l999, ^{186}Os-^{187}Os systematics of Hawaiian picrites: Earth and Planetary Science Letters, v. 174, p. 25-42.

Cumming, V.M., Poulton, S.W., Rooney, A.D., Selby, D., 2013, Anoxia in the terrestrial environment during the late Mesoproterozoic: Geology, v. 41, p. 583-586.

Gramlich, J.W., Murphy, T.J., Garner, E.L., Shields, W.R., 1973, Absolute isotopic abundance ratio and atomic weight of a reference sample of rhenium: Journal of Research of the National Bureau of Standards. Section A: Physics and Chemistry, v. 77A, p. 691-698.

Kendall, B.S., Creaser, R.A., Ross, G.M., Selby, D., 2004, Constraints on the timing of Marinoan "Snowball Earth" glaciation by ^{187}Re-^{188}Os dating of a Neoproterozoic post-glacial black shale in Western Canada: Earth and Planetary Science Letters, v. 222, p. 729-740.

Kendall, B.S., Creaser, R.A., and Selby, D., 2009, ^{187}Re-^{188}Os geochronology of Precambrian organic-rich sedimentary rocks: Geological Society of London Special Publications, v. 326, p. 85-107.

Ludwig, K.R., 1980, Calculation of uncertainties of U-Pb isotope data: Earth and Planetary Science Letters, v. 46, p. 212-220.

Ludwig, K.R., 2011, Isoplot/Ex, Version 4.15: A geochronological toolkit for Microsoft Excel: Geochronology Center Berkeley, v. 4, p. 1-70. http://www.bgc.org/isoplot_etc/isoplot.html.

Rooney, A.D., Selby, D., Houzay, J.-P., Renne, P.R., 2010, Re-Os geochronology of a Mesoproterozoic sedimentary succession, Taoudeni basin, Mauritania: Implications for basin-wide correlations and Re-Os organic-rich sediments systematics: Earth and Planetary Science Letters, v. 289, p. 486-496.

Rooney, A.D., Chew, D.M., Selby, D., 2011, Re-Os geochronology of the Neoproterozoic-Cambrian Dalradian Supergroup of Scotland and Ireland: Implications for Neoproterozoic stratigraphy, glaciation and Re-Os systematics: Precambrian Research, v. 185, p. 202-214.

Selby, D., and Creaser, R.A., 2003, Re-Os geochronology of organic-rich sediments: an evaluation of organic matter analysis methods: Chemical Geology, v. 200, p. 225-240.

Smoliar, M.I., Walker, R.J., Morgan, J.W., 1996, Re-Os ages of Group IIA, IIIA, IVA and IVB iron meteorites: Science, v. 271, p. 1099-1102.

van Acken, D., Brandon, A.D., Lapen, T.J., 2012. Highly siderophile element and osmium isotope evidence for postcore formation magmatic and impact processes on the aubrite parent body: Meteoritics and Planetary Science, v. 47, p. 1606-1623.

Wittig, N., Humayun, M., Brandon, A.D., Huang, S., Leya, I., 2013. Coupled W-Os-Pt systematics of IVB iron meteorites: In situ neutron dosimetry for W isotope chronology: Earth and Planetary Science Letters, v. 361, p. 152-161.

Table DR1: Carbonate Carbon, Organic Carbon and Oxygen isotopes of the upper Callison Lake Dolostone

Section	Stratigraphic Height (m)	$\delta^{13}C_{carb}$ (‰)	$\delta^{18}O_{carb}$ (‰)	$\delta^{13}C_{org}$ (‰)	Epsilon (‰)	Siliclastic Content (%)	Carbonate Content (%)	TOC (%)
J1204	0.3	4.00	-2.84	–	–	–	–	–
J1204	1	3.91	-3.11	–	–	–	–	–
J1204	1.3	3.61	-5.12	–	–	–	–	–
J1204	2	3.77	-4.16	–	–	–	–	–
J1204	2.5	3.61	-4.36	–	–	–	–	–
J1204	3	3.78	-2.45	–	–	–	–	–
J1204	3.4	3.15	-2.96	–	–	–	–	–
J1204	4.1	2.58	0.35	–	–	–	–	–
J1204	4.4	2.26	-0.19	–	–	–	–	–
J1204	5	2.01	-0.93	–	–	–	–	–
J1204	5.5	1.67	0.42	–	–	–	–	–
J1204	6.1	1.63	0.11	–	–	–	–	–
J1204	6.5	1.29	-0.19	–	–	–	–	–
J1204	7	0.73	0.31	–	–	–	–	–
J1204	7.4	0.01	0.92	–	–	–	–	–
J1204	8	1.05	1.33	–	–	–	–	–
J1204	8.3	0.58	1.00	–	–	–	–	–
J1204	19.3	-2.78	-1.19	–	–	–	–	–
J1204	20	-2.67	-1.22	–	–	–	–	–
J1204	20.4	-4.02	-1.56	–	–	–	–	–
J1204	20.9	-3.77	-0.94	–	–	–	–	–
J1204	21.1	-3.60	-0.62	–	–	–	–	–
J1204	21.9	-7.00	-1.30	–	–	–	–	–
J1204	22.3	-2.76	-4.21	–	–	–	–	–
J1204	22.9	-4.21	-1.87	–	–	–	–	–
J1204	23.3	-3.96	-2.01	–	–	–	–	–
J1204	23.9	-3.94	-2.07	–	–	–	–	–
J1204	24.4	-4.07	-2.22	–	–	–	–	–
J1204	25.4	-2.88	-5.85	–	–	–	–	–
J1204	25.9	-6.53	-2.16	–	–	–	–	–
J1204	27.2	-5.64	-2.07	–	–	–	–	–
J1204	27.5	-5.50	-1.89	–	–	–	–	–
J1204	29.6	-3.26	-0.82	–	–	–	–	–
J1204	30.9	-2.97	-2.95	–	–	–	–	–
J1204	32.2	-2.37	-0.28	–	–	–	–	–
F930	2	3.73	-3.65	-25.14	28.87	9.62	90.25	0.13
F930	3	3.38	-1.71	-29.19	32.58	13.82	86.07	0.11
F930	5	2.30	-0.08	-26.93	29.23	13.42	86.44	0.14
F930	6	1.61	0.33	-30.50	32.11	10.20	89.72	0.09
F930	8	1.15	-0.40	-30.08	31.22	13.16	86.74	0.09
F930	9	-0.98	0.98	-31.18	30.20	23.08	76.73	0.19
F930	16	-3.31	-0.16	-31.22	27.91	6.37	93.58	0.04
F930	18	-6.77	-1.91	-31.53	24.76	10.03	89.86	0.11
F930	20	-4.55	-2.72	-27.68	23.13	27.58	72.33	0.09
F930	21	-5.88	-1.88	-30.11	24.23	4.41	95.50	0.08
F930	22	-3.89	0.03	-28.16	24.27	3.64	96.29	0.07
F930	23	-4.83	-0.62	-28.88	24.05	2.01	97.95	0.04
F930	25	-1.39	-0.14	-32.87	31.48	41.57	58.41	0.01
F930	26	-1.62	-0.39	-34.99	33.36	45.42	54.55	0.03

F930-2–9 m = J1204-0.3–8.3 m and F930-16–26m = J1204-19.3–32.2 m

Table DR2: Re and Os abundance and isotope composition data for the Callison Lake Dolostone

Sample	Isochron point	Re (ppb)	±	Os (ppt)	±	^{192}Os (ppt)	±	^{187}Re / ^{187}Os	±	^{187}Os/^{188}Os	±	rho[a]	Os initial[b]
16.8	A	0.71	0.01	61.8	0.2	21.8	0.1	64.6	1.1	1.421	0.016	0.489	0.620
17.7#1	B	3.29	0.02	138.8	0.4	44.0	0.1	148.8	1.0	2.453	0.013	0.659	0.608
17.7#2	C	1.93	0.01	80.3	0.3	25.4	0.1	151.5	1.5	2.479	0.022	0.732	0.600
17.7#3	D	3.55	0.02	174.1	0.8	56.9	0.1	124.1	1.0	2.152	0.032	0.395	0.613
17.7#4	E	5.67	0.02	203.3	2.1	63.9	0.4	182.8	0.5	2.880	0.018	0.668	0.613
17.7#5	F	9.51	0.04	357.6	4.9	77.9	0.3	171.8	0.5	2.738	0.029	0.384	0.608
17.7#6	G	4.71	0.03	159.7	1.8	53.6	0.3	196.2	0.7	3.050	0.022	0.617	0.617
17.7#7	H	4.87	0.02	178.3	1.8	42.2	0.1	177.5	0.5	2.814	0.017	0.680	0.612
18.1	I	1.87	0.01	92.6	0.3	30.3	0.2	123.1	1.1	2.131	0.015	0.704	0.605
18.2	J	1.68	0.01	148.3	0.5	52.6	0.1	63.4	0.7	1.393	0.015	0.462	0.606

Uncertainties are given as 2σ for ^{187}Re/^{188}Os, ^{187}Os/^{188}Os and ^{192}Os

For the latter the uncertainty includes the 2 SE uncertainty for mass spectrometer analysis plus uncertainties for Os blank abundance and isotopic composition.

Ages are calculated using the $\lambda^{187}Re = 1.666 \times 10^{-11} y^{r-1}$ (Smoliar et al., 1996).

a Rho is the associated error correlation (Ludwig, 1980)

b Os initial = ^{187}Os/^{188}Os isotope composition calculated at 739 Ma

Table DR3: Locations where VSMs have been described in the literature (after Porter and Knoll, 2000). Age constraints are rough and noted from italisized references when neccessary.

Formation/Rock Unit	Location	Paleocontinent	Relationship to Islay anomaly?	Approximate Age	Reference
A. Assemblages with multiple VSM species in common:					
Backlundtoppen Formation	Spitsbergen, Svalbard	Laurentia	Older	780–716 Ma	Knoll et al. (1989); *Halverson et al. (2004)*
Callison Lake Dolostone	Yukon, Canada	Laurentia	Yes	ca. 740 Ma	This paper
Draken Formation	Spitsbergen, Svalbard	Laurentia	Older	780–716 Ma	Knoll et al. (1991); *Halverson et al. (2004)*
Chuar Group	Grand Canyon, Arizona	Laurentia	Older?	785–742 Ma	Bloeser (1985); Porter et al. (2003); *Karlstrom et al. (2000); Dehler et al. (2012)*
Beck Springs Dolomite	Death Valley, California	Laurentia	Yes	770–716 Ma	Licari (1978); Horodyski (1993); *Macdonald et al. (2013); Mahon et al. (2014)*
Russøya Member, Elbobreen Formation	Nordhaustlandet, Svalbard	Laurentia	Yes	780–716 Ma	Knoll and Calder (1983); *Halverson et al. (2004)*
Uinta Mountain Group	Uinta Mountains, Utah	Laurentia	Older?	785–716 Ma	Link et al. (1993); *Dehler et al. (2010)*
B. Assemblages with broad morphological similarity to the Callison Lake Dolostone, but with distinct taxa or insufficient systematic research					
Bed 18, Eleonore Bay Group	East Greenland	Laurentia	Unknown	780–716 Ma	Vidal (1979); Green et al. (1988); *Hoffman et al. (2012)*
Chatkaragai Suite	Tien Shan, Russia/Kyrgyzstan	Kazakstan	Unknown	800–766 Ma	Kraskov (1985); Yankaouskas (1989); *Sergeev and Schopf (2010); Meert et al. (2011)*
Chichkan Formation	Kazakstan	Kazakstan	Unknown	800–766 Ma	Sergeev and Schopf (2010); *Meert et al. (2011)*
Jabal Rockham	Saudi Arabia	Arabia	Unknown	>650 Ma	Binda and Bokhari (1980); *Johnson (2003)*
Togari Group	Tasmania	Australia	Yes	780–716 Ma	Saito et al. (1988); *Turner et al. (1998)*
Visingsö Beds	Sweden	Baltica	Unknown	805–663 Ma	Ewetz (1933); Knoll and Vidal (1980); *Vidal and Siedlecka (1983); Martí Mus and Moczydlowska (2000)*
C. Reported vasiform microfossils that are distinct from the Callison Lake Dolostone, insufficiently illustrated, or poorly preserved					
Bonahaven Formation, Dalradian Supergroup	Scotland	Laurentia?	Younger	665–635 Ma	Anderson et al. (2013)
Dengying Formation	China	South China	Younger	551–542 Ma	Zhang and Li (1991); Ding et al. (1992); Duan et al. (1993); Zhang (1994); *Condon et al. (2005)*
Doushantuo Formation	China	South China	Younger	635–551 Ma	Duan (1986); Duan et al. (1993); Li et al. (2008); *Condon et al. (2005)*
Jacadigo Group	Brazil	Amazonia	Younger	716–635 Ma	Fairchild et al. (1978); *Freitas et al. (2011)*
Rasthof Formation	Namibia	Congo	Younger	665–635 Ma	Bosak et al. (2011)
Simla Slates	India	India	Unknown	823–716 Ma	Nautiyal (1978); *Jiang et al. (2003)*
Tanafjorden Group	Norway	Baltica	Unknown	807–716 Ma	Vidal and Siedlecka (1983); *Vidal and Moczydlowska (1995)*
Tindir Group	Alaska	Laurentia	Unknown	811–716 Ma	Allison and Awramik (1994); *Macdonald et al. (2010)*
Tsagaan Oloom Formation	Mongolia	Mongolia	Younger	665–635 Ma	Bosak et al. (2011)
Upper Min'yar Formation	Urals, Russia	Baltica	Unknown	820–687 Ma	Maslov et al. (1994); *Maslov (2004)*
Vaishnodevi Limestone	Himalaya, India	India	Unknown	<950 Ma	Venkatachala and Kumar (1998); *McKenzie et al. (2011)*
Vindhyan Supergroup	India	India	Unknown	>650 Ma?	Maithy and Babu (1988); *Ray et al. (2002)*
Virgin Springs Limestone	Death Valley, California	Laurentia	Younger	740–716 Ma	Macdonald et al. (2013); *This paper*

References

Allison, C.W., and Awramik, S.M., 1989, Organic-walled microfossils from the earliest Cambrian or latest Proterozoic Tindir Group rocks, Northwest Canada: Precambrian Research, v. 43, p. 253–294.
Anderson, R.P., Fairchild, I.J., Tosca, N.J., and Knoll, A.H., 2013, Microstructures in metasedimentary rocks from the Neoproterozoic Bonahaven Formaton, Scotland: Microconcretions, impact spherules, or microfossils?: Precambrian Research, v. 233, p. 59–72.
Binda, P.L., and Bokhari, M.M., 1980, Chitinozoanlike microfossils in a late Precambrian dolostone from Saudi Arabia: Geology, v. 8, p. 70-71.
Bloeser, B., 1985, *Melanocyrillium*, a new genus of structurally complex Late Proterozoic microfossils from the Kwagunt Formation (Chuar Group), Grand Canyon, Arizona: Journal of Paleontology, v. 59, p. 741–765.
Bosak, T., Lahr, D.J.G., Pruss, S.B., Macdonald, F.A., Dalton, L., and Matys, E., 2011, Agglutinated tests in post-Sturtian cap carbonates of Namibia and Mongolia: Earth and Planetary Science Letters, v. 308, p. 29–40.
Condon, D., Zhu, M., Bowring, S., Wang, W., Yang, A., and Jin, Y., 2005, U-Pb ages from the Neoproterozoic Doushantuo Formation, China: Science, v. 308, p. 95–98.
Dehler, C.M., Fanning, C.M., Link, P.K., Kingsbury, E.M., and Rybczynski, D., 2010, Maximum depositional age and provenance of the Uinta Mountain Group and Big Cottonwood Formation, northern Utah: Paleogeography of rifting western Laurentia: Geological Society of America Bulletin, v. 122, no. 9-10, p. 1686–1699.
Dehler, C.W., Karlstrom, K.E., Gehrels, G.E., Timmons, M.J., and Crossey, L.J., 2012, Stratigraphic revision, provenance, and new age constraints on the Nankoweap Formation and Chuar Group, Grand Canyon Supergroup, Grand Canyon, Arizona: Geological Society of America Abstracts with Programs, v. 44, no. 6, p. 82.
Ding, L.F., Zhang, L.Y., Li, Y., Dong, J.S., 1992, The study of the late Sinian–Early Cambrian biota from the northern margin of Yangtze Platform: Scientific and Technical Documents Publishing House, Beijing, p. 1–156.
Duan, C., 1985, The earliest Cambrian vase-shaped microfossils of Fangxian County, Hubei Province: Bulletin of the Tianjin Institute of Geology and Mineral Resources, v. 13, p. 87–107.
Duan, C., Cao, F., and Zhang, L., 1993, Vase-shaped microfossils from the top of the Tongying Formation in Xixiang, Shaanxi: Acta Micropaleontologica, v. 10, p. 397–408.
Ewetz, C.E., 1933, Einige neue Fossilfunde in der Visingsöformation: Geologiska Föreningens I Stockholm Förhandlingar, v. 55, p. 506–518.
Fairchild, T.R., Barbour, A.P., and Haralyi, N.L.E., 1978, Microfossils in the 'Eopaleozoic' Jacadigo Group at Urucum, Mato Grosso, southwest Brazil: Boletim IG, v. 9, p. 74–79.
Freitas, B.T., Warren, L.V., Boggiani, P.C., Paes De Almeida, R., and Piacentini, T., 2011, Tectono-sedimentary evolution of the Neoproterozic BIF-bearing Jacadigo Group, SW Brazil: Sedimentary Geology, v. 238, p. 48–70.
Green, J.W., Knoll, A.H., and Swett, K., 1988, Microfossils from oolites and pisolites of the upper Proterozoic Eleonore Bay Group, Central East Greenland: Journal of Paleontology, v. 62, p. 835–852.
Halverson, G.P., Maloof, A.C., and Hoffman, P.F., 2004, The Marinoan glaciation (Neoproterozoic) in northeast Svalbard: Basin Research, v. 16, p. 297–324.
Hoffman, P.F., Halverson, G.P., Domack, E.W., Maloof, A.C., Swanson-Hysell, N.L., and Cox, G.M., 2012, Cryogenian glaciations on the southern tropical paleomargin of Laurentia (NE Svalbard and East Greenland), and a primary origin for the upper Russøya (Islay) carbon isotope excursion: Precambrian Research, v. 206-207, p. 137-158.
Horodyski, R.J., 1993, Paleontology of Proterozoic shales and mudstones: examples from the Belt Supergroup, Chuar Group, and Pahrump Group, western USA: *in* B. Nagy, J.S. Leventhal, and R.F. Grant, eds., Metalliferous black shales and related ore deposits: Precambrian Research, v. 61, p. 241–278.
Jiang, G., Sohl, L.E., and Christie-Blick, N., 2003, Neoproterozoic stratigraphic comparison of the Lesser Himalaya: Geology, v. 31, no. 10, p. 917–920.
Johnson, P.R., 2003, Post-amalgamation basins of the NE Arabian shield and implications for Neoproterozoic III tectonism in the northern East African orogen: Precambrian Research, v. 123, p. 321–337.
Karlstrom, K.E., Bowring, S.A., Dehler, C.M., Knoll, A.H., Porter, S.M., Marais, Des, D.J., Weil, A.B., Sharp, Z.D., Geissman, J.W., Elrick, M.B., Timmons, J.M., Crossey, L.J., and Davidek, K.L., 2000, Chuar Group of the Grand Canyon: Record of breakup of Rodinia, associated change in the global carbon cycle, and ecosystem expansion by 740 Ma: Geology, v. 28, no. 7, p. 619–622.
Knoll, A.H., and Calder, S., 1983, Microbiota of the Late Precambrian Ryssö Formation, Nordaustlandet, Svalbard: Palaeontology, v. 26, p. 467-496.
Knoll, A.H., and Vidal, G., 1980, Late Proterozoic vase-shaped microfossils from the Visingsö Beds, Sweden: Geologiska Föreningens i Stockholm Förhandlingar, v. 102, p. 207–211.
Knoll, A.H., Swett, K., and Burkhart, E., 1989, Paleoenvironmental distribution of microfossils and stromatolites in the Upper Proterozoic Backlundtoppen Formation, Spitsbergen: Journal of Paleontology, v. 63, p. 129–145.
Knoll, A.H., Swett, K., and Mark, J., 1991, Paleobiology of a Neoproterozoic tidal flat/lagoonal complex: the Draken Conglomerate Formation, Spitsbergen: Journal of Paleontology, v. 65, p. 531–570.
Kraskov, L.N., 1985, Nakhodka problematichnikh organizmov votlozheniykh chatkaragaikoii sviti (Talasskii khrebet): *in*, A.M. Obut and N.J. Tchernysheva, eds., Problematika pozdnego dokembriya I paleozoya, p. 149–152.
Li, Y., Guo, J., Zhang, X., Zhang, W., Liu, Y., Yang, W., Li, Y., Liu, L., and Shu, D., 2008, Vase-shaped microfossils from the Ediacaran Weng'an biota, Guizhou, South China: Gondwana Research, v. 14, no. 1-2, p. 263-268.
Licari, G.R., 1978, Biogeology of the late pre-Phanerozoic Beck Springs Dolomite of eastern California: Journal of Paleontology, v. 52, p. 767–792.
Link, P.K., Christie-Blick, N., Devlin, W.J., Elston, D.P., Horodyski, R.J., Levy, M., Miller, J.M.G., Pearson, R.C., Prave, A., Stewart, J.H., Winston, D., Wright, L.A., Wrucke, C.T., 1993, Middle and Late Proterozoic stratified rocks of the western U.S. Cordillera, Colorado Plateau, and Basin and Range province: in, J.C. Reed Jr., M.E. Bickford, R.S. Houston, P.K. Link, D.W. Rankin, P.K. Sims, and W.R. Van Schmus, eds., The geology of North America: Geological Society of America, Boulder, CO, p. 463–595.
Macdonald, F.A., Halverson, G.P., Strauss, J.V., Smith, E.F., Cox, G.M., Sperling, E.A., and Roots, C.F., 2010, Early Neoproterozoic basin formation in Yukon, Canada: Implications for the make-up and break-up of Rodinia: Geoscience Canada, v. 39, p. 77-99.
Macdonald, F.A., Prave, A., Petterson, R., Smith, E.F., Pruss, S., Oates, K., Waechter, F., Trotzuk, D., and Fallick, A., 2013, The Laurentian record of Neoproterozoic glaciation, tectonism, and eukaryotic evolution in Death Valley, California: Geological Society of America Bulletin, v. 125, no. 7-8, p. 1203–1223.
Mahon, R.C., Dehler, C.M., Link, P.K., Karlstrom, K.E., and Gehrels, G.E., 2014, Geochronologic and stratigraphic constraints on the Mesoproterozoic and Neoproterozoic Pahrump Group, Death Valley, California: A record of the assembly, stability, and break of Rodinia: Geological Society of America Bulletin, v. XXX, p. XXX.
Maithy, P.K., and Babu, R., 1988, Chitinozoa-like remains from Vindhyan Supergroup of Son Valley: Palaeobotanist, v. 37, p. 77–80.
Martí Mus, M., and Moczydlowska, M., 2000, Internal morphology and taphonomic history of the Neoproterozoic vase-shaped microfossils from the Visingsö Group, Sweden: Norsk Geologisk Tidsskrift, v. 80, p. 213–228.
Maslov, A.V., Abduazimova, Z.M., Karsten, L.A., and Puchkov, V.N., 1994, Pervye nakhodki *Mellanoserillium* v etalonnykh rifeya na Yuzhnon Urale: Sostoyanie, problemy I zadachi geologicheskogo kartirovaniya oblastei rasvitiya dokembrya na territorii Rossi, p. 90–91.
Maslov, A.V., Riphean and Vendian sedimentary sequences of the Timanides and Uralides, the eastern periphery of the East European Craton: Geological Society of London Memoirs, v. 30, p. 19–35.
McKenzie, N.R., Hughes, N.C., Myrow, P.M., Xiao, S., and Sharma, M., 2011, Correlation of Precambrian–Cambrian sedimentary successions across northern India and utility of isotopic signatures of Himalayan lithotectonic zones: Earth and Planetary Science Letters, v. 312, p. 471–483.
Meert, J.G., Gibsher, A.S., Levashova, N.M., Grice, W.C., Kamenov, G.D., and Ryabinin, A.B., 2011, Glaciation and ~770 Ma Ediacara (?) fossils from the Lesser Karatau Microcontinent, Kazakhstan: Gondwana Research, v. 19, p. 867–880.
Nautiyal, A.C., 1978, Discovery of cyanophycean remains and chitinozoans from the late Precambrian argillaceous sequence of Satpuli, Garhwal Himalaya, India: Current Science, v. 47, p. 222–226.
Porter, S.M., Meisterfield, R., and Knoll, A.H., 2003, Vase-shaped microfossils from the Neoproterozoic Chuar Group, Grand Canyon: A classification guided by modern testate amoebae: Journal of Paleontology, v. 77, no. 3, p. 409–429.
Ray, J.S., Martin, M.W., Veizer, J., and Bowring, S.A., 2002, U-Pb zircon dating and Sr isotope systematics of the Vindhyan Supergroup, India: Geology, v. 30, no. 2, p. 131–134.
Saito, Y., Tiba, T., and Matsubara, S., 1988, Precambrian and Cambrian cherts in Northwestern Tasmania: Bulletin of the National Science Museum, Tokyo, v. 14, p. 59–70.
Sergeev, V.N., and Schopf, J.W., 2010, Taxonomy, paleoecology, and biostratigraphy of the Late Neoproterozoic Chichkan microbiota of south Kazakhstan: The marine biosphere on the even of metazoan radiation: Journal of Paleontology, v. 84, no. 3, p. 363–401.
Turner, N.J., Black, L.P., and Kamperman, M., 1998, Dating of Neoproterozoic and Cambrian orogenies in Tasmania: Australian Journal of Earth Science, v. 45, no. 5, p. 789–806.
Venkatachala, B.S., and Kumar, A., 1998, Fossil microbiota from the Vaishnodevi Limestone, Himalayan Foothills, Jammu: age and paleoenvironmental implications: Journal of the Geological Society of India, v. 52, p. 529–536.
Vidal, G., 1979, Acritarchs from the Upper Proterozoic and Lower Cambrian of East Greenland: Grønlands Geologiske Undersøgelse Bulletin, v. 131, p. 1–55.
Vidal, G., and Moczydlowska, M., 1995, The Neoproterozoic of Baltica–stratigraphy, palaeobiology, and general geological evolution: Precambrian Research, v. 28, p. 197–216.
Vidal, G., and Siedlecka, A., 1983, Planktonic, acid-resistant microfossils from the Upper Proterozoic strata of the Barents Sea Region of Varanger Peninsula, East Finmark, Northern Norway: Norges Geologiske Undersokelse, v. 382, p. 45–79.
Yankaouskas, T.V., ed., 1989, Mikrofossilii dokembriia SSSR, Nauka, Leningrad.
Zhang, L.Y., 1994, A new progress in research on vase-shaped microfossils from the Dengying Formation of Sinian in southern Shaanxi Province: Acta Geologica Gansu, v. 13, p. 1–8.
Zhang, L., and Li, Y., 1991, The Late Sinian vasiform microfossils of Ningqiang, Shaanxi Province: Bulletin of the Xi'an Institute of Geological and Mineralogical Research: Chinese Academy of Geological Sciences, v. 31, p. 77–86.